

DiffH₂O: Diffusion-Based Synthesis of Hand-Object Interactions from Textual Descriptions

SAMMY CHRISTEN*, ETH, Switzerland and Meta, Switzerland
 SHREYAS HAMPALI, Meta, Switzerland
 FADIME SENER, Meta, Switzerland
 EDOARDO REMELLI, Meta, Switzerland
 TOMAS HODAN, Meta, Switzerland
 ERIC SAUSER, Meta, Switzerland
 SHUGAO MA, Meta, United States of America
 BUGRA TEKIN, Meta, Switzerland

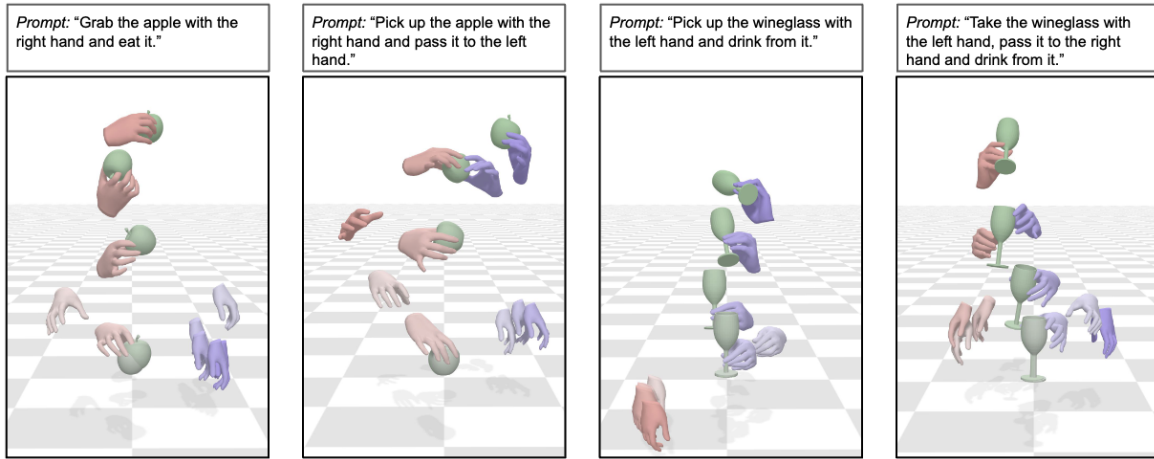


Fig. 1. We introduce DiffH₂O, a diffusion-based framework to synthesize dexterous hand-object interactions. DiffH₂O generates realistic hand-object motion from natural language, generalizes to unseen objects at test time and enables fine-grained control over the motion with detailed textual descriptions. Time is visualized with a color code where lighter shades denote the past. Best seen in the supplemental video.

We introduce DiffH₂O, a new diffusion-based framework for synthesizing realistic, dexterous hand-object interactions from natural language. Our model employs a temporal two-stage diffusion process, dividing hand-object motion generation into grasping and interaction stages to enhance generalization to various object shapes and textual prompts. To improve generalization to

*This work was done during an internship at Meta.

Authors' Contact Information: Sammy Christen, sammychristen@gmail.com, ETH, Switzerland and Meta, Switzerland; Shreyas Hampali, hampali@meta.com, Meta, Switzerland; Fadime Sener, famesener@meta.com, Meta, Switzerland; Edoardo Remelli, edoremelli@meta.com, Meta, Switzerland; Tomas Hodan, tomhodan@meta.com, Meta, Switzerland; Eric Sauser, esouser@meta.com, Meta, Switzerland; Shugao Ma, shugao@meta.com, Meta, United States of America; Bugra Tekin, bugratekin@meta.com, Meta, Switzerland.

Permission to make digital or hard copies of all or part of this work for personal or classroom use is granted without fee provided that copies are not made or distributed for profit or commercial advantage and that copies bear this notice and the full citation on the first page. Copyrights for components of this work owned by others than the author(s) must be honored. Abstracting with credit is permitted. To copy otherwise, or republish, to post on servers or to redistribute to lists, requires prior specific permission and/or a fee. Request permissions from [permissions@acm.org](https://www.acm.org/permissions).

SA Conference Papers '24, December 3–6, 2024, Tokyo, Japan

© 2024 Copyright held by the owner/author(s). Publication rights licensed to ACM.

ACM ISBN 979-8-4007-1131-2/24/12

<https://doi.org/10.1145/3680528.3687563>

unseen objects and increase output controllability, we propose grasp guidance, which directs the diffusion model towards a target grasp, seamlessly connecting the grasping and interaction stages through a motion imputation mechanism. We demonstrate the practical value of grasp guidance using hand poses extracted from images or grasp synthesis methods. Additionally, we provide detailed textual descriptions for the GRAB dataset, enabling fine-grained text-based control of the model output. Our quantitative and qualitative evaluations show that DiffH₂O generates realistic hand-object motions from natural language, generalizes to unseen objects, and significantly outperforms existing methods on a standard benchmark and in perceptual studies.

CCS Concepts: • **Computing methodologies** → **Procedural animation**.

Additional Key Words and Phrases: motion generation, dexterous manipulation, hand-object interaction, diffusion models

ACM Reference Format:

Sammy Christen, Shreyas Hampali, Fadime Sener, Edoardo Remelli, Tomas Hodan, Eric Sauser, Shugao Ma, and Bugra Tekin. 2024. DiffH₂O: Diffusion-Based Synthesis of Hand-Object Interactions from Textual Descriptions. In *SIGGRAPH Asia 2024 Conference Papers (SA Conference Papers '24)*, December 3–6, 2024, Tokyo, Japan. ACM, New York, NY, USA, 15 pages. <https://doi.org/10.1145/3680528.3687563>

1 Introduction

Modeling and understanding hand-object interactions (HOI) is an important and crucial task to empower machines to interact with and assist humans. Being able to seamlessly generate hand-object motions holds the promise to enable synthetic data generation [Leonardi et al. 2023], assist robots in training human-robot interactions in simulation, or enhance realism in virtual manipulation experiences. For example, in virtual reality (VR), hand interactions still often rely on heuristics and controllers that simply attach objects to the hand according to pre-defined grasps. Being able to faithfully produce object manipulation based on an input signal such as text or a few past frames of hand and object poses could largely increase the immersiveness of such interactions.

Generating realistic hand-object interactions in 3D is challenging as the resulting motions are required to be plausible in several different aspects. First, the motions must be plausible in terms of *geometry*, such that hand and object intersections are minimized and the grasp appears stable. Second, the motions must be plausible in terms of *semantics*, such as the hands respect natural object affordances (e.g., a cup is grasped by its handle and not flipped upside down). Third, the motions must be plausible in terms of *time*, such as the hand and object motions are synchronized and the dynamics appear natural. Another challenge in generating HOI comes from the limited scale of existing hand-object datasets, which are around 10x smaller than human motion datasets [Mahmood et al. 2019] and 1000x smaller than image datasets [Deng et al. 2009].

Several recent works have successfully leveraged diffusion models for full-body human motion generation but either neglect objects [Karunratanakul et al. 2023; Tevet et al. 2023] or focus only on coarse motion of larger objects (e.g., a chair) without finger predictions [Xu et al. 2023a]. Another method, IMoS [Ghosh et al. 2023], generates HOI with smaller objects (e.g., a cup or stapler) by first predicting upper-body motions and then optimizing object poses in post-processing. However, IMoS assumes that the object is in-hand from the beginning, handles only objects seen during training, and, as shown in our experiments, often yields artifacts (e.g., hand-object interpenetration or non-plausible contacts). In this paper, we aim to learn a model that *generates natural, fine-grained hand-object interactions and generalize to objects unseen during training*.

Towards this goal, we contribute a novel diffusion-based framework, DiffH₂O, that generates hand-object interactions based on text prompts and geometry of the object. We propose several techniques to deal with the challenges of data scarcity and object generalization.

Decoupling Grasping and Interaction: Hand-object interactions can be invariably split into a grasping phase where the hand(s) approaches the static object for grasping, and an interaction phase where the object is manipulated based on an action intent. For example, drinking from a cup can be performed with multiple grasps, and given a grasp, multiple actions are possible. We use this simple observation to obtain a grasping and an interaction diffusion model, and introduce an inpainting technique called subsequence imputing to allow continuity between the two outputs. In contrast to previous diffusion frameworks that employ coarse-to-fine (trajectory-to-full motion) motion generation [Karunratanakul et al. 2023], we split the task temporally and propose a temporal two-stage diffusion

model. **Pose Representation:** We introduce a compact representation that models hands in parametric space. To couple the hands to the object, we represent the global hand positions relative to the normalized object position at the initial frame, and further include distance information between the 3D hand joints and the object surface. While encoding distances helps reason about local shape, representing coordinates relative to the initial frame allow us to better adjust to unseen object geometry compared to per-frame object-relative pose representation used in existing work [Christen et al. 2022]. **Controllability:** We provide two ways to add more control to our diffusion models’ output. First, we propose control through fine-grained textual descriptions. To this end, we contribute textual descriptions to the GRAB dataset [Taheri et al. 2020] and show that they enable more robustness to unseen test prompts and increase controllability, e.g., by allowing to prompt the interacting hand and the action to perform. Second, when a target grasp reference pose for a given object is available, we propose to leverage it to connect the grasping and interaction phases by guiding our two diffusion models at inference time. The grasp reference provides a prior about how and with which hand an object should be grasped. It can either be obtained from from an image-based pose estimator [Pavlakos et al. 2024] or grasp synthesis [Zhang et al. 2024a] as we show in our experiments in Section 5.7.

To demonstrate the effectiveness of our approach, we run perceptual studies and experiments on the GRAB dataset [Taheri et al. 2020]. We first compare against IMoS [Ghosh et al. 2023]. Our results indicate that our method generates better results across a variety of physics-based and motion metrics. To justify our technical contributions, we compare our final model against human-body diffusion baselines by adapting these methods to HOI. We show that we generate motions of higher quality while enabling more control of the outputs reaching feasible poses. Furthermore, we demonstrate that detailed textual descriptions increase robustness to unseen texts and offer better control of the diffusion model than training with heuristics-generated text descriptions. Decoupling our method into two stages and grasp guidance brings better generalization and high practical value to DiffH₂O through controllability, e.g., for downstream tasks such as animation or generating synthetic data at scale. We show this with two applications for grasp guidance: i) using an image-based pose estimator [Pavlakos et al. 2024] and ii) leveraging pre-generated grasp poses [Zhang et al. 2024a] to define target reference grasps, and consequently sampling multiple different actions through text in the interaction stage.

We contribute the following: **(i)** To the best of our knowledge, DiffH₂O is the first method that synthesizes hand-object interactions on unseen objects from textual descriptions. **(ii)** A temporal two-stage diffusion process that splits generation into grasping and action-based interaction, which improves generalization to different textual prompts. **(iii)** Grasp guidance and subsequence imputing that can be applied at inference to the diffusion process to increase the controllability of outputs and improve generalization to unseen objects. **(iv)** Detailed textual descriptions to the GRAB dataset. Code and data will be made public upon acceptance*.

*For code and data, see our project website here: <https://diffh2o.github.io>

2 Related Work

2.1 Hand-Object Synthesis

Recent efforts in interaction synthesis have largely been driven by the surge of high-quality human-object interaction datasets [Brahmbhatt et al. 2019, 2020; Chao et al. 2021; Fan et al. 2023; Hampali et al. 2020; Hasson et al. 2019; Kwon et al. 2021; Liu et al. 2022; Taheri et al. 2020; Wang et al. 2023; Yang et al. 2022; Zhan et al. 2024]. Some studies focus on generating coarse full-body object interactions [Hassan et al. 2023; Lee and Joo 2023; Luo et al. 2021; Wang et al. 2021; Zhang et al. 2022a], such as carrying boxes. FLEX [Tendulkar et al. 2023] trains a hand and body pose prior and optimizes the priors to achieve diverse, static full-body grasps. GOAL [Taheri et al. 2022] and SAGA [Wu et al. 2022] use CVAEs to generate approaching motions for full-body grasps, whereas TOHO [Li et al. 2024b] models both approaching and manipulation tasks via neural implicit representations. Similarly, Braun et al. [2024] model the full range of motion, leveraging physics simulation and reinforcement learning (RL). In contrast, we focus on fine-grained HOI and generalization to unseen objects. Among methods that model full-body object interaction, closest to our work is IMoS [Ghosh et al. 2023], a two-stage method to generate HOI on seen objects based on language prompts. Starting from a grasping state, they first generate body motions and then optimize for object trajectories using a heuristics-based optimization to model HOI. By contrast, our model directly predicts the hand and object poses, models both approaching and manipulation, and generalizes to unseen objects.

Another line of research focuses on generation of hand-object interaction sequences in isolation from full-body due to wide applications in VR and the need for a dedicated model for fine-grained details of finger motion. One prominent solution is to turn to physical simulation and RL, e.g., by learning dexterous manipulation tasks in simulation from full human demonstration data either collected via teleoperation [Rajeswaran et al. 2018] or from videos [Garcia-Hernando et al. 2020; Qin et al. 2021]. Mandikal and Grauman [2021] propose a reward function that incentivizes dexterous robotic hand policies to grasp in the affordance region of objects. Li et al. [2024a] propose a solution for grasping multiple objects at once. She et al. [2022] propose a new dynamic state representation to generate dexterous grasps, whereas other works leverage implicit representation [Karunratanakul et al. 2020] or force-closure [Liu et al. 2021]. D-Grasp [Christen et al. 2022] and Unidexgrasp [Xu et al. 2023b] leverage RL and physics simulation to generate diverse hand-object interactions from sparse reference inputs. ArtiGrasp [Zhang et al. 2024b] extends this to two-handed grasps and generates articulated object motions. Unidexgrasp++ [Wan et al. 2023] proposes a solution that transfers to vision-based inputs, which may be used for robotic grasping. These works focus on achieving stable grasping, whereas we model both the grasping and manipulation of objects.

To model HOI, another solution is to rely on purely data-driven frameworks. For example, [Liu and Yi 2024; Taheri et al. 2024; Zhou et al. 2022] propose methods that enable denoising hand-poses from noisy sequences of hand-object poses. Ye and Liu [2012] predict the local hand pose given full body and object motion. Similarly, ManipNet [Zhang et al. 2021] predicts local hand poses for two-handed interactions based on wrist-object trajectories. Given object

motion of articulated objects, CAMS [Zheng et al. 2023] predicts one-handed poses that align with the object motion, whereas Chen et al. [2023b] focus on grasping objects using dexterity in the environment. All these works either assume a hand-object trajectory, focus only on one hand, ignore semantic action information, or do not generalize well to unseen objects. In contrast, we propose a framework that allows the synthesis of two-handed object interactions from text as well as generalization to unseen objects.

2.2 Diffusion for Motion Synthesis

Diffusion models [Sohl-Dickstein et al. 2015] have gained popularity in many domains such as image generation [Ho et al. 2020], video generation [Yang et al. 2023], audio synthesis [Kong et al. 2021] or hand reconstruction [Ye et al. 2023a,b]. They have also been adapted to human motion synthesis [Tevet et al. 2023; Zhang et al. 2022b]. Various improvements have been proposed by integrating physics [Yuan et al. 2023], scene-awareness [Huang et al. 2023], increasing efficiency by diffusing in a pre-trained latent space [Chen et al. 2023a], or the composition of multiple actions [Athanasios et al. 2022]. To enable more controllability during motion synthesis, Karunratanakul et al. [2023] propose GMD that guides the diffusion model towards target objectives at inference time. However, GMD contains design choices specific to human motion generation, by first generating a 2D root trajectory over the whole sequence, and then generating corresponding full-body poses, which is not directly transferable to HOI. While these works focus on human motion in isolation from objects, InterDiff [Xu et al. 2023a] generates human-object interactions via diffusion models. Their work is improved upon by recent concurrent works [Diller and Dai 2023; Li et al. 2023; Peng et al. 2023] that leverage contact-based predictions in combination with inference time-guidance to improve the interaction quality. However, these works focus on full-body motions and neglect intricate hand-object interactions. In contrast, we focus on the detailed interactions of fingers and objects. Most similar to ours, the concurrent work MACS [Shimada et al. 2023] proposes a diffusion model for hand-object motion synthesis. Their focus is on synthesizing interactions for a single object with varying mass, while our focus is on generalization to unseen shapes and interaction synthesis conditioned on text.

3 Preliminary: Diffusion Models

Denoising Diffusion Probabilistic Models (DDPM) [Sohl-Dickstein et al. 2015] model the probability distribution of a given dataset for images [Rombach et al. 2022], videos [Ho et al. 2022] or motion sequences [Tevet et al. 2023]. The diffusion model involves a forward process, which is a Markov chain consisting of sequentially adding Gaussian noise to the data, and a reverse process to denoise the data gradually. The forward process results in a distribution, $q(\mathbf{x}_t|\mathbf{x}_{t-1})$, where a clean input \mathbf{x}_0 is gradually noised to \mathbf{x}_T , with $t \in [0, T]$ as the total number of diffusion steps. The reverse process models the probability distribution, $p_\theta(\mathbf{x}_{t-1}|\mathbf{x}_t)$, where the noisy input \mathbf{x}_T is denoised into \mathbf{x}_0 , which is modeled via a neural network with parameters θ . The process of data generation involves sequential denoising and noising steps. The denoising is modeled in auto-encoder fashion predicting either directly the denoised output,

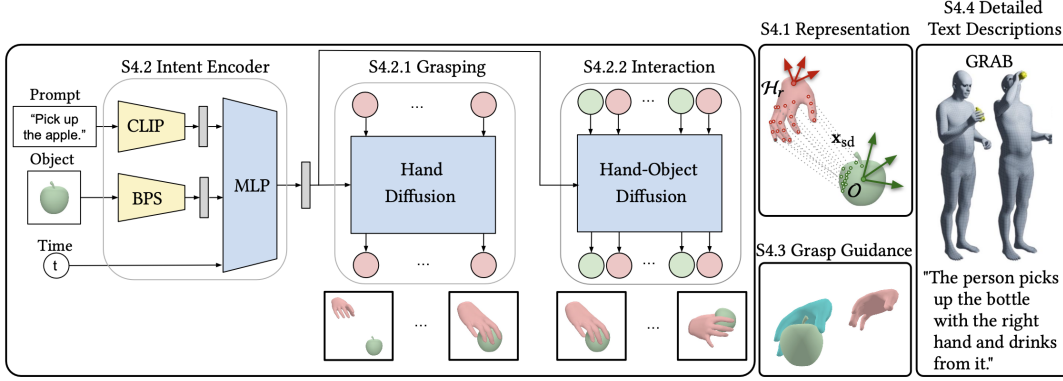


Fig. 2. **Overview of DiffH₂O.** We couple hands and objects by representing hands relative to the object position in the initial frame and encoding hand-object distances (Sec. 4.1). We observe that objects are static until they have been grasped, and propose to decouple grasping and interaction stages and modelling them with two different diffusion processes (Sec. 4.2). Finally, we make use of grasp guidance and subsequence imputation to ensure a smooth transition between these two stages (Sec. 4.2.3). We further show fine-grained synthesis controllability through our detailed textual descriptions (Sec. 4.4).

$\mathbf{x}_{0,\theta}(\mathbf{x}_t, t)$; the mean, $\boldsymbol{\mu}_\theta(\mathbf{x}_t, t)$, or the noise, $\boldsymbol{\epsilon}_\theta(\mathbf{x}_t, t)$, used in the noising process. The auto-encoder is trained to minimize

$$\mathcal{L}_{\text{Diff}} = \mathbb{E}_{\boldsymbol{\epsilon} \sim \mathcal{N}(0,1), t} \mathcal{L}_{ae}, \quad (1)$$

where \mathcal{L}_{ae} is either $\|\mathbf{x}_{0,\theta}(\mathbf{x}_t, t) - \mathbf{x}_0\|$, $\|\boldsymbol{\mu}_\theta(\mathbf{x}_t, t) - \boldsymbol{\mu}\|$, or $\|\boldsymbol{\epsilon}_\theta(\mathbf{x}_t, t) - \boldsymbol{\epsilon}\|_2^2$. Depending on the application, a different choice of the model output works better in practice, e.g., directly predicting the output \mathbf{x}_0 for human motion [Tevet et al. 2023] or guidance [Karunratanakul et al. 2023]. Conditional diffusion models generate output conditioned on various kinds of input such as text [Rombach et al. 2022] or other semantic information [Zhang et al. 2023]. Such a model is obtained by providing the condition as additional signal, \mathbf{c} , to the auto-encoder, resulting in outputs $\mathbf{x}_{0,\theta}(\mathbf{x}_t, t, \mathbf{c})$, $\boldsymbol{\mu}_\theta(\mathbf{x}_t, t, \mathbf{c})$, or $\boldsymbol{\epsilon}_\theta(\mathbf{x}_t, t, \mathbf{c})$.

Diffusion models can be guided to generate outputs of the required form. Two popular methods to guide the diffusion models are classifier guidance [Dhariwal and Nichol 2021] and classifier-free guidance [Ho and Salimans 2022]. We describe the classifier-free guidance method here and refer the reader to [Ho and Salimans 2022] for details on classifier-free guidance. The classifier-free guidance method approximates $p_\theta(\mathbf{x}_{t-1} | \mathbf{x}_t, \mathbf{c}) \propto p_\theta(\mathbf{x}_{t-1} | \mathbf{x}_t) p(\mathbf{c} | \mathbf{x}_t)$, where \mathbf{c} is the guidance signal. Deriving from this, Dhariwal and Nichol [2021] show that the new sampling process can be expressed as

$$\boldsymbol{\mu}_\theta(\mathbf{x}_t, t) = \boldsymbol{\mu}_\theta(\mathbf{x}_t, t)' + s\beta \nabla_{\mathbf{x}_t} \log p(\mathbf{c} | \mathbf{x}_t), \quad (2)$$

where $\boldsymbol{\mu}_\theta(\mathbf{x}_t, t)'$ indicates the original mean, s is the scaling of the gradients, and β is a variance scheduler. Here the mean is shifted by the scaled gradient. Intuitively, the scaled gradient of the guidance signal, $\nabla_{\mathbf{x}_t} \log p(\mathbf{c} | \mathbf{x}_t)$ nudges the denoised mean $\boldsymbol{\mu}_\theta$ to generate samples in accordance with the guidance \mathbf{c} . $\log p(\mathbf{c} | \mathbf{x}_t)$ could represent the class probability which can be implemented using a neural-net, or could represent a cost term $G(\mathbf{x}_t)$ that is optimized. The classifier guidance method has the advantage that it can use pre-trained diffusion models without retraining them and can benefit from any guidance signal that is differentiable to guide the diffusion.

4 Method

We focus on the task of generating a sequence of hand and object poses $\mathbf{x} := (\mathcal{H}_l, \mathcal{H}_r, \mathcal{O})$, where $(\mathcal{H}_l, \mathcal{H}_r)$ indicate a sequence of left and right hand poses, and \mathcal{O} is a sequence of object poses given some input conditioning signal \mathbf{c} , which in our case comprises a text description and the object mesh. In other words, we want to model a conditional probability distribution $p(\mathbf{x} | \mathbf{c}, G = 0)$ with a motion DDPM. The optional term $G = 0$ can be any differentiable goal function that should be minimized, e.g., the distance to a target grasp in our case (see Sec. 4.3). See Fig. 2 for an overview. In Sec. 4.1, we introduce our compact representation that couples the hand and object poses. We propose a two-stage generation of hand-object interactions in Sec. 4.2 and grasp guidance in Sec. 4.3. Lastly, in Sec. 4.4, we introduce our newly-collected detailed textual annotations for GRAB that enable more controlled generation of HOI.

4.1 Canonicalized Hand-Object Representation

Our proposed canonicalized representation $\mathbf{x} = (\mathcal{O}, \mathcal{H}_l, \mathcal{H}_r) \in \mathbb{R}^N$, where N is the number of steps in the sequence, contains information about both hands and an object. The object poses are defined as $\mathcal{O} = (\boldsymbol{\tau}_o, \boldsymbol{\phi}_o)$, where $\boldsymbol{\tau}_o := (\boldsymbol{\tau}_o^0, \boldsymbol{\tau}_o^1, \dots, \boldsymbol{\tau}_o^{N-1})$ is a sequence of 3D object locations, with $\boldsymbol{\tau}_o^i \in \mathbb{R}^3$, and $\boldsymbol{\phi}_o := (\boldsymbol{\phi}_o^0, \boldsymbol{\phi}_o^1, \dots, \boldsymbol{\phi}_o^{N-1})$ is a sequence of 3D object orientations, with $\boldsymbol{\phi}_o^i \in \mathbb{R}^6$ in 6D representation [Zhou et al. 2019]. The hands are represented by: $\mathcal{H}_j = (\boldsymbol{\tau}, \boldsymbol{\phi}, \boldsymbol{\theta}, \mathbf{x}_{sd})$, $j \in \{l, r\}$, where l denotes the left and r the right hand, respectively. This representation is based on the parametric MANO hand model [Romero et al. 2017]. Specifically, the global 3D positions of the hands are given by $\boldsymbol{\tau} \in \mathbb{R}^{3 \times N}$ and the global 3D orientations are represented by $\boldsymbol{\phi} \in \mathbb{R}^{6 \times N}$. To achieve more natural poses, we define the local hand pose in PCA space of MANO with the first 24 components as $\boldsymbol{\theta} \in \mathbb{R}^{24 \times N}$. We further encode signed distances, $\mathbf{x}_{sd} \in \mathbb{R}^{21 \times 3 \times N}$, between each hand joint and its closest point on the object mesh. As we show in ablations (see Tab. 4), this approximation of a signed-distance field (SDF), coupled with our diffusion model reduces physical artifacts. Existing works [Christen et al. 2022] encode hand-object poses with a per-frame object-relative

representation, which tightly couples the hands to the training object pose and therefore limits generalization to unseen objects. In contrast, we represent hand positions relative to the normalized object position at the frame that marks the boundary between the grasp and interaction stage. This representation is less variant to specific training object pose and more correlated with the global poses involved in HOI, which is often shared across different training objects in HOI datasets [Chao et al. 2021; Taheri et al. 2020]. As a result, it yields better generalization and accuracy for HOI across different (unseen) objects, as we show in ablations in Sec. 5.6.

4.2 Two-Stage Hand-Object Generation

We split the synthesis into grasping and interaction stages to facilitate generalization to unseen objects. The grasping stage models the motion from an initial pose to object grasp. The interaction stage performs an action-based manipulation of the object. Our two-phase approach is motivated by the fact that any hand-object interaction involves an approaching phase where one or two hands grasp a static object, followed by an intent-driven interaction with the object. By decoupling the action-based manipulation from grasping, we can leverage the entire set of motions in the data for training the grasping phase, irrespective of the action that is performed in the interaction phase. These insights help counteract the limited scale of the data and improve generalization to different textual inputs.

As shown in Fig. 2, our grasping and interaction diffusion models are conditioned on three types of inputs, namely, 1) text prompts describing the object and the action to be carried out, 2) object mesh which provides the geometry of the object, and 3) the time step t in the denoising process. We use CLIP [Radford et al. 2021] embeddings to encode the text prompt denoted by \mathcal{T} , BPS [Prokudin et al. 2019] to encode the object mesh denoted by \mathcal{M} and an MLP to encode the time step as in previous works [Dhariwal and Nichol 2021]. We provide more implementation details in supplementary material and describe the grasping and interaction phases below in detail.

4.2.1 Grasping Stage. This stage is defined as a sequence containing one or two hands approaching a static object from a rest pose until the object is grasped. As the object is static throughout this phase we do not predict the object motion and only model the hand pose sequence. To obtain the training data for this phase we use heuristics to determine sequence boundaries from the larger action sequences. In particular, the boundary is defined as the first frame where the object’s lateral and vertical velocity surpass a threshold of 0.01m/s and at least 7 vertices of the hand are in contact with the object. We then normalize the sequence lengths by interpolating or downsampling the poses. The text description in this phase is a generic sentence ("The person grasps the <object>").

We use the ϵ_θ diffusion model that directly predicts the noise in classifier-free manner [Ho and Salimans 2022] which is more suitable for inference-time guidance [Karunratanakul et al. 2023], e.g., grasp guidance (Section 4.2.3). In other words, our grasping diffusion model training loss is given by

$$\mathbb{E}_{\epsilon \sim \mathcal{N}(0,1), t} \|\epsilon_\theta(\mathbf{x}_t^g, \mathcal{T}, \mathcal{M}, t) - \epsilon\|_2^2, \quad (3)$$

where \mathbf{x}_t^g is the synthesized motion at diffusion step t and the final output of the grasping stage after denoising \mathbf{x}_t^g with ϵ_θ is \mathbf{x}_0^g .

4.2.2 Interaction Stage. This stage comprises the motion of both hands and the object after a grasp has been established. The hands manipulate and interact with the object according to the action defined through the textual prompt. We use the same sequence boundary determined in the grasping stage to get the training data for interaction. We employ a \mathbf{x}_0 diffusion model in a classifier-free manner (see Section 3), i.e., we directly predict the denoised output \mathbf{x}_0^i , that result in less noisy, higher quality motion than ϵ_θ diffusion model for the interaction phase that does not involve inference-time grasp guidance. Our training loss is given by

$$\mathbb{E}_{\epsilon \sim \mathcal{N}(0,1), t} \|\mathbf{x}_{0,\theta}^i(\mathbf{x}_t^i, \mathcal{T}, \mathcal{M}, t) - \mathbf{x}_0^i\|_2^2. \quad (4)$$

4.2.3 Grasp to Interaction Stage Transition. Maintaining a seamless transition between the grasping and interaction outputs is critical to generating realistic motion sequences. We utilize motion imputing on the interaction model to achieve a smooth transition. In particular, we impute the start of the interaction sequence from the entire sequence obtained by the (guided) grasping model. Intuitively, this adjusts the generative process for interaction stage based on the observed grasping motion. To perform the imputation, we define the projection P_g^i that resizes the hand poses $\mathbf{x}_0^g \in (\mathcal{H}_l, \mathcal{H}_r)$ from the grasping stage to hand-object poses \mathbf{x}_0^i from the interaction stage by filling in zeros, both temporally and spatially. Similarly, M_g^i represents the imputation regions of the grasp sequence on \mathbf{x}_0^i . At each denoising step, the imputed denoised output $\tilde{\mathbf{x}}_{0,\theta}^i$ is given by

$$\tilde{\mathbf{x}}_{0,\theta}^i = (1 - M_g^i) \odot \mathbf{x}_{0,\theta}^i + M_g^i \odot P_g^i \mathbf{x}_0^g, \quad (5)$$

where \odot is elementwise multiplication. Our proposed technique, dubbed *subsequence imputing*, leads to smoother transition between grasp & interaction compared to single frame transition (see Sec. 5.6).

4.3 Grasp Guidance

To add controllability to the generation and improve generalization to unseen objects, we introduce grasp guidance for the grasping stage, which can be optionally added at inference time via the goal function G (see Sec. 3 and Eq. 2). We leverage a single grasp frame $\hat{\mathbf{h}}_0^g$ as target grasp (hand pose) for the last frame of the grasping stage. It provides a prior about how and with which hand an object should be grasped. Such a grasp can be obtained from grasp generation [Zhang et al. 2024a] or from an off-the-shelf hand-object pose estimator [Pavlakos et al. 2024] as demonstrated in Sec. 5.7. We aim to minimize the goal function $G(\mathbf{x}_t^g) = 0$ and approximate the gradient of the guidance signal in Eq. 2 as

$$\nabla_{\mathbf{x}_t^g} \log p(\mathbf{c}|\mathbf{x}_t^g) = -\nabla_{\mathbf{x}_t^g} G(\mathbf{x}_t^g) \approx -\nabla_{\mathbf{x}_t^g} \|\mathbf{h}_{0,\theta}^g(\mathbf{x}_t^g) - \hat{\mathbf{h}}_0^g\|_2^2, \quad (6)$$

where $\mathbf{h}_{0,\theta}^g \in (\mathcal{H}_l, \mathcal{H}_r)$ is the hand(s) pose in the last frame of the grasping sequence after denoising \mathbf{x}_t^g and the cost term $G(\mathbf{x}_t^g)$ minimizes the distance of the hand(s) pose to the target grasp. Depending on the availability, the guidance signal may include one or two hands. Since the diffusion process is a denoising model of a motion sequence, it relates individual frames to other frames in the sequence. Hence, by backpropagating through the diffusion model (via autograd), we can compute a dense guidance signal for all frames, even if only sparse guidance signals (one in our case) are provided.

4.4 Detailed Text Descriptions

Our model generates hand-object interactions based on textual inputs. To the best of our knowledge, there is currently no HOI dataset that contains detailed textual descriptions. For instance, the GRAB dataset [Taheri et al. 2020] only provides categorical action labels. To address this, we auto-generated sentences using the template “the person <verb> + <object>” [Ghosh et al. 2023] (referred to as “simple” text). However, these sentences lack detailed information, which limits the controllability of the model via textual inputs. Therefore, we contribute carefully annotated textual descriptions of GRAB (referred to as “detailed” sentences). We instructed our annotators to carefully watch each ground truth video and describe the actions in three distinct stages of *pre-action*, *action*, and *post-action*. These descriptions are further augmented with hand and positional information. An example from the dataset is as follows: “The person picks up the apple with the right hand, passes it to their left hand, and places it back with their right hand”. These detailed descriptions enhance the dataset, enabling more accurate generation and precise control of HOI as we show in Sec. 5.8.

5 Experiments and Results

5.1 Baselines

Our method focuses on synthesizing detailed hand-object motion based on text input. To the best of our knowledge, DiffH₂O is the first method to tackle this problem. While there is no direct baseline for hand-object motion synthesis based on language, the closest to our approach is IMoS [Ghosh et al. 2023], which focuses on text-based whole-body human-object interaction synthesis. IMoS first generates a body articulation based on an instruction label (action + object), and then optimizes for the object pose using a grasp heuristic. Since our paper focuses on hand articulations and object motions, we omit the full-body movements from our evaluations.

To further compare DiffH₂O against human-body diffusion models, such as [Tevet et al. 2023] and [Karunratanakul et al. 2023], we adopted them to the HOI setting. All variants use our proposed pose representation. MDM [Tevet et al. 2023] does not use guidance, and for GMD [Karunratanakul et al. 2023], we use gradients to guide the model towards the grasp frame, but omit the 2D-trajectory generation stage because it is specific to human motions.

5.2 Data

5.2.1 GRAB. We utilize the subject-based split of the GRAB dataset [Taheri et al. 2020], which contains 1335 sequences, proposed in IMoS to run a direct comparison. However, as this split does not contain unseen objects, we also create a new split featuring unseen objects based on object similarity and semantics (see supplemental material). To assess our model’s ability to generalize to unseen classes, we introduce a new split comprising unseen objects that were not present in training. Our train and test split contains 1125 and 210 sequences, respectively, which we mirror to a total of 2250 and 420 sequences. To split the GRAB sequences into the grasping and interaction stages for training, we apply the heuristics described in Section 4.2.1 Our test set is composed of the following objects: “apple, mug, train, elephant, alarm clock, small pyramid, medium

cylinder and large torus”. Note that the training set includes pyramids, cylinders, and torus in other sizes. We exclude small pyramids, medium cylinders, and large torus from the training set to test our models’ ability to generalize to different sizes of the same objects to evaluate grasp guidance in a controlled manner, we utilize the frame of the unseen test split that indicates the transition between the grasp and interaction stage. Note that the grasp reference contains both hands in this case, even if one hand is not grasping the object.

5.2.2 HO-3D. To further evaluate guidance and object generalization, we estimate poses on the HO-3D dataset [Hampali et al. 2020] and guide our model to an estimated target hand pose.

5.3 Evaluation Metrics

We report several physics-based metrics and motion diversity metrics following previous works [Braun et al. 2024; Ghosh et al. 2023; Taheri et al. 2022; Tendulkar et al. 2023]. Please see supplementary material for additional metrics based on action features.

5.3.1 Physics Based Metrics. We report the interpenetration volume (IV) as the number of MANO vertices penetrating the object mesh and the maximum interpenetration depth (ID). Additionally, we compute the contact ratio (CR) as the average ratio of hand vertices within 5mm of the object mesh.

5.3.2 Motion Metrics. We report the sample diversity (SD) between wrist trajectories in motion space. We sample the same input conditions 5 times, compute the pairwise Euclidean distance between the samples and report the mean SD over all test prompts. We also provide the overall diversity (OD), which measures the pairwise Euclidean distance between all test samples. Furthermore, we report the action recognition accuracy (AR) as in [Ghosh et al. 2023].

5.3.3 Guidance Metrics. To assess how well the models adhere to the guidance signal, we report the mean error between the predictions and the reference grasp (GE), and the ratio at which the diffusion model maintains the correct handedness according to the reference (HA). Furthermore, we evaluate the wrist velocities at the transition between grasping and interaction phase (T_{vel}).

5.4 Comparison to the State-of-the-Art

We conduct a set of experiments to compare to relevant baselines quantitatively. We present qualitative examples of our method in Fig. 4 and failure cases in Fig. 5.

5.4.1 Setting 1 - Interaction Only. We compare our approach against the closest existing work, IMoS, in their interaction-only setting and report results in Tab. 1. To ensure a fair comparison with IMoS, we evaluate our model without the grasp guidance and without our detailed text annotations. We test DiffH₂O with two backbones, transformer as in [Tevet et al. 2023] and UNet as in [Karunratanakul et al. 2023]. Our model significantly outperforms IMoS across all physics and motion diversity metrics. In particular, our method yields motions that are significantly more diverse (higher SD and OD), exhibit less interpenetration (lower IV and ID), and align better with the action type (higher AR). Note that IMoS assumes the availability of a ground-truth test motion to initialize the first few frames, while ours predicts the entire sequence. Yet, our approach

Table 1. **Comparison to State-of-the-Art in the Interaction Stage.** We compare our method with two backbones (transformer and UNet) against IMoS [Ghosh et al. 2023]. We report results on an unseen subject split (top 3 rows) [Ghosh et al. 2023], and on our unseen object test dataset (bottom 3 rows). For IMoS, we use the same pretrained model, trained on unseen subject split, across all our experiments (unseen subject/object splits), due to difficulties in reproducing training performance for the unseen object split (indicated with IMoS* in the table). †: higher values are better, ‡: lower values are better.

	Method	Backbone	SD [m] (†)	OD [m] (†)	IV [cm ³] (‡)	ID [mm] (‡)	CR (†)	AR (†)
Unseen subject split	IMoS [Ghosh et al. 2023]	CVAE	0.002	0.149	7.14	11.47	0.05	0.588
	DiffH ₂ O	Transformer	0.088	0.185	6.65	8.39	0.067	0.810
	DiffH ₂ O	UNet	0.109	0.188	6.02	7.92	0.064	0.875
Unseen object split	IMoS* [Ghosh et al. 2023]	CVAE	0.002	0.132	10.38	12.45	0.048	0.581
	DiffH ₂ O	Transformer	0.133	0.185	7.99	10.87	0.073	0.803
	DiffH ₂ O	UNet	0.134	0.179	9.03	11.39	0.086	0.837

Table 2. **Comparison to Diffusion Baselines for the Full Sequence.** We compare against HOI-adapted versions of MDM and GMD. We measure the grasp error (GE) and the accuracy of handedness (HA) with respect to the reference grasp, the interpenetration volume (IV), and the wrist joint velocities (T_{vel}) at the transition between grasping and interaction.

Method	IV [cm ³] (‡)	GE [m] ‡	HA †	T_{vel} [$\frac{m}{s}$] ‡
MDM	8.98	0.38	0.45	0.14
GMD	7.47	0.30	0.58	0.20
Ours	7.40	0.12	0.87	0.23

achieves considerable performance improvements. While IMoS provides compelling realistic full body synthesis results, fine-grained finger motions and object motions lag behind the realism and diversity demonstrated by our method, as shown in Fig. 3 and in our supplementary video. In Section 5.5, we further provide a perceptual study to compare our method against the baseline.

5.4.2 Setting 2 - Grasping + Interaction. In this experiment, we focus on generating entire sequences of grasping and interaction, evaluating how well the models can produce high-quality motions without physical artifacts and adhere to guidance signals. Results in Tab. 2 show our method outperforms human motion diffusion baselines (MDM/GMD) with better grasp accuracy (GE), handedness (HA), and naturalness (IV). This validates our temporal two-stage design with grasp guidance and subsequence imputing over previous diffusion models for the setting of hand-object interactions.

5.5 Perceptual User Study

To evaluate the visual quality of our motions, we conducted a perceptual user study on a set of 21 participants, who were randomly assigned one of four sets, each consisting of 30 randomly selected sequences. We compared our approach against IMoS. We displayed results from our method and IMoS side-by-side in random order, along with the input sentence description used to synthesize motions. We asked the following questions to the participants: “Which sequence is more realistic?” and “Which sequence has more variety in motion?”. We defined a sequence to be more realistic if the overall motion looks human-like, e.g., if the object is grasped realistically and there are less artifacts such as floating objects or

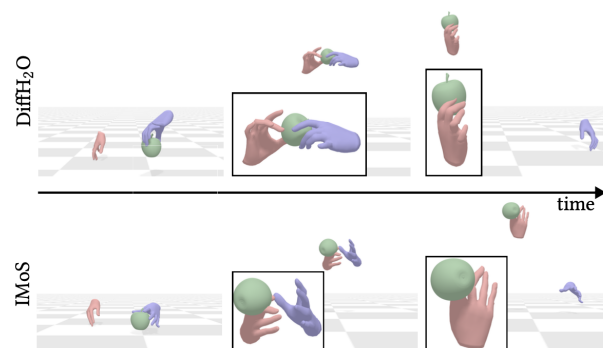


Fig. 3. **Qualitative Comparison.** Post-optimizing object motion as in IMoS [Ghosh et al. 2023] (bottom row) exhibits artifacts with fine-grained manipulations, e.g., when an object switches hands. In contrast, our approach (top row) seamlessly handles such cases. Best seen in supplemental video.

interpenetration. Moreover, a sequence has more variety if the object is manipulated multiple times and in distinct ways. In 63.1% of the responses, participants selected our method as the most realistic compared to IMoS. Even more distinctively, in 72.9% of the responses, participants favored our method to contain more variety than IMoS. We obtained statistically significant Fleiss’ kappa scores [Fleiss 1971] of 0.34 and 0.43 for Realism and Diversity, respectively, at $p < 0.05$. In our investigation, our model showed low realism but high diversity for the “pass” action, influenced by users perceiving “pass” action label in the GRAB dataset as transferring an object between hands, not to another person. In the “offhand” action category of GRAB, where an object is passed from one hand to another (see Figure 3 and video 02:51), our model excelled in realism, while IMoS exhibited artifacts. This is due to the fact that IMoS determines the hand which is in contact with the object according to ground-truth, which leads to a jump of the object for the “off-hand” category.

5.6 Ablation Studies

We perform several ablations to justify our technical contributions. To evaluate the controllability gained through guidance, we compare our final method with several variants in Tab. 3 for the full setting that generates the whole sequence with grasping and interaction (Setting 2). We use a base model which indicates a single

Table 3. **Ablation Study.** We provide ablations of our components against the base model. We measure the grasp error (GE) and the accuracy of handedness (HA) with respect to the reference grasp, as well as interpenetration volume (IV). We also provide the wrist joint velocities (T_{vel}) for the transition from grasping to interaction. Bold is the best, underlined is the second best.

Component			Metrics			
2-ST	GG	SI	IV [cm^3] ↓	GE [m] ↓	HA ↑	T_{vel} [$\frac{m}{s}$] ↓
×	×	×	7.48	0.31	0.52	0.21
✓	×	×	9.03	0.49	0.46	12.68
✓	✓	×	8.52	0.06	0.97	5.37
✓	✓	✓	7.40	<u>0.12</u>	<u>0.87</u>	<u>0.23</u>

stage model without guidance. We then gradually add our model components: (i) 2-stage design that decouples grasping and interaction (2-ST), (ii) grasp guidance (GG), and, (iii) subsequence imputing in the interaction phase (SI) as described in Sec. 4.2. As expected, the grasp reference is being ignored without guidance (top 2 rows in Tab. 3), leading to high grasp errors and low hand correctness. Adding guidance allows for better performance in grasp error and hand accuracy, however, a high T_{vel} indicates a sudden jump of the hands between grasping and interaction. Our subsequence imputing mitigates this and leads to the best overall score at the cost of a slight increase in grasp error and decrease in hand correctness. The IV is lowest with our final model, indicating the best generalization to unseen objects. To validate our representation, we further compare our approach, which normalizes hands with respect to the object position at first frame, against a number of baselines: (i) a variant inspired by D-Grasp [Christen et al. 2022] that involves a redundant representation involving joint angles in Euler space and angular velocities, (ii) our representation without SDF, and, (iii) our representation with per-frame object relative poses. As shown in Tab. 4, our final representation achieves the best overall scores and trade-off with low interpenetration and high contact ratios. As discussed in Sec. 4.1, our representation relative to initial frame is less variant with specific object shapes and more correlated with motion involved in hand-object interaction compared to per-frame object-relative representation. This effectively improves generalization for HOI across different objects. In addition, SDF feature further improves accuracy by reasoning about local shape.

The D-Grasp representation has the lowest interpenetration scores, but as indicated by the contact ratio and our qualitative results in the video, the hands are often disconnected from the objects, potentially due its challenge in optimizing in high-dimensional, redundant feature space. Additionally, our PCA space helps reduce unnatural hand poses that occur when predicting joints in angle space directly (see supplemental video). While the PCA space is beneficial in data-sparse settings, it may hinder more fine-grained finger manipulations compared to joint angle predictions.

5.7 Generation from Estimated and Pre-Synthesized Pose

We show two qualitative applications of DiffH₂O in video. First, we run an image-based pose estimator [Pavlakos et al. 2024] on single images from HO3D [Hampali et al. 2020] to obtain object-relative hand poses. Second, we generate grasping poses using GraspXL [Zhang et al. 2024a]. We then pass these hand poses through our

Table 4. **Pose Representation Evaluation.** We compare different alternative pose representations in interaction stage and demonstrate the benefits of object-relative pose representation and encoding hand-object signed distances. Bold indicates the best result, underlined is the 2nd best result.

Pose Representation (unseen objects)	Metrics		
	CR ↑	IV [cm^3] ↓	ID [mm] ↓
D-Grasp [Christen et al. 2022]	0.055	5.56	8.60
Ours w/o SDF	0.073	10.79	11.42
Ours w/ object-relative pose	<u>0.077</u>	9.38	11.41
Ours w/ first frame relative pos. (Ours)	0.086	<u>9.03</u>	<u>11.39</u>

method as reference grasps in grasp guidance (see Sec. 4.3), together with multiple different textual descriptions. This highlights the practicality of our framework given a single grasp reference or grasp motion, to generate multiple diverse sequences. See supplementary material for details about how we obtain grasp references and further discussions on their benefits and limitations.

5.8 Controllability via Text Prompts

In this experiment, we train DiffH₂O once with our detailed text descriptions and once with simple text prompts generated from the GRAB objects and action labels. We measure whether the active hand in the generated motion corresponds to the prompted hand to gauge controllability. Results in Tab. 5 show that detailed text descriptions significantly improve control over handedness, achieving an accuracy of 86.5% vs. 59.3% with simple prompts. Performance drop when training on simple texts and testing on detailed texts (0.702) and vice-versa, which was similarly observed in [Shvetsova et al. 2023] due to a style gap. We also measure action correctness by evaluating action recognition accuracy (AR, see Sec. 5.3). Using detailed descriptions enables our model to generate motions that align more accurately with the text input, demonstrated by a 0.887 action accuracy compared to 0.516 with our model tested with simple prompts. Since the test inputs are much more diverse with the detailed textual descriptions, this furthermore demonstrates the robustness to unseen sentences. We also report the cosine similarity between the different sets of texts as a reference.

Table 5. **Text evaluation.** We demonstrate that detailed text descriptions enable us to generate motions more representative of the description, and allow fine-grained controllable hand-object motion synthesis.

Train Input	Test Input	AR	Hand correctness				Cosine Similarity
			Right	Left	Both	Total	
simple	simple	0.837	n/a	n/a	n/a	n/a	0.72
detailed	simple	0.516	n/a	n/a	n/a	n/a	0.43
simple	detailed	0.702	0.709	0.111	0.0	0.593	0.43
detailed	detailed	0.887	0.869	0.862	0.75	0.865	0.66

6 Discussion and Conclusion

We have introduced a framework to generate plausible hand-object interactions from textual descriptions. Specifically, we have proposed a two-stage diffusion framework that decouples sequences into grasping and interaction, and can use single grasps as guidance to the diffusion model to improve generalization to unseen objects.

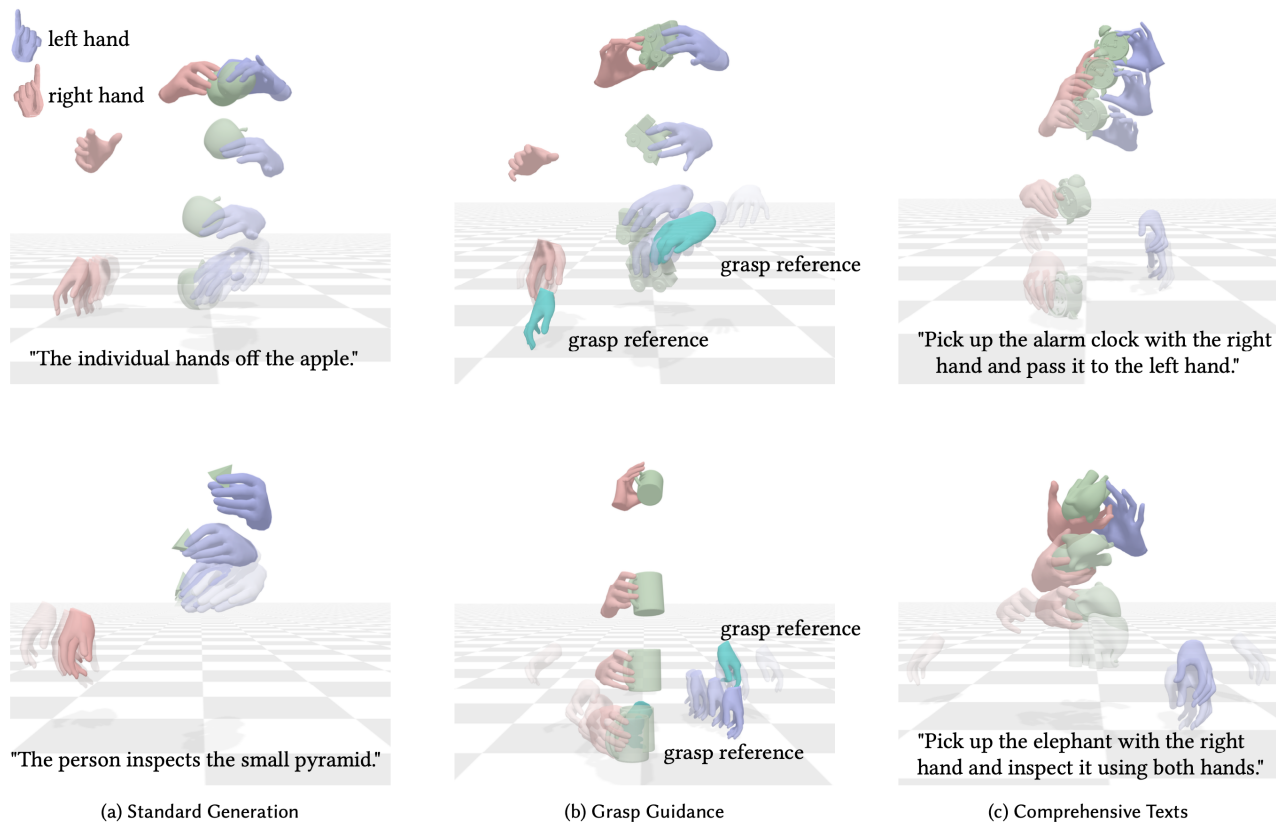


Fig. 4. **Qualitative Examples.** We provide more qualitative examples with a) standard generation without any guidance b) grasp guidance c) our model trained with detailed text descriptions.

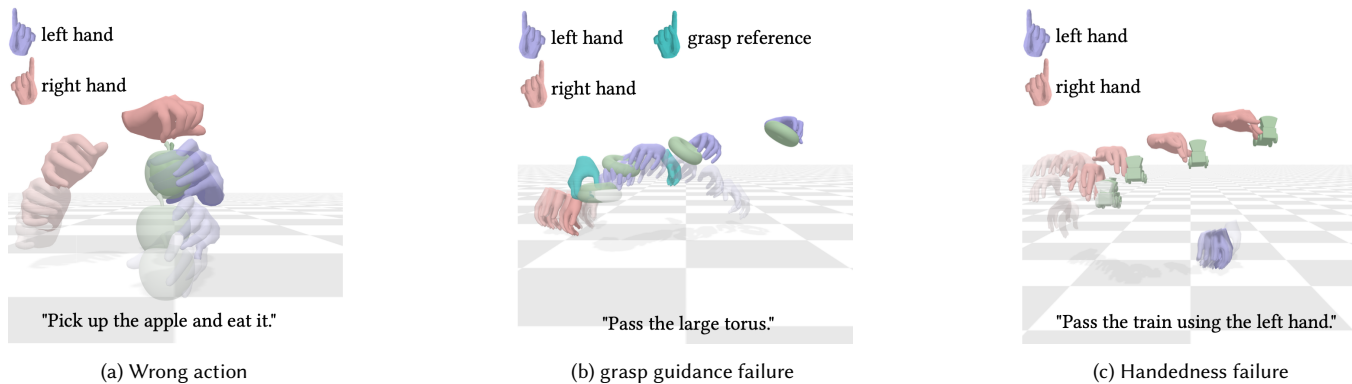


Fig. 5. **Failure Cases.** We present three possible failure cases of our method. a) The generated motion does not match the action described in the input prompt, such as trying to perform a bottle opening motion with an apple. b) During grasp guidance, the reference grasp is largely ignored in the diffusion process, resulting in an interaction that is distinct from the grasp reference. c) Despite training with our curated text annotations, the model sometimes does not pick up on the cue of handedness and may interact with a hand different from the one provided in the text prompt.

While we provide a first step towards HOI synthesis generalization, there are limitations of our framework. To remove physical artifacts, physics could be explicitly integrated into the diffusion

process [Yuan et al. 2023]. The inference time is still relatively slow. To increase efficiency, operating in latent space is an interesting direction to explore [Chen et al. 2023a].

References

- Nikos Athanasiou, Mathis Petrovich, Michael J Black, and Gül Varol. 2022. Teach: Temporal action composition for 3d humans. In *International Conference on 3D Vision (3DV)*. IEEE, 414–423.
- Samarth Brahmabhatt, Cusuh Ham, Charles C Kemp, and James Hays. 2019. Contactdb: Analyzing and predicting grasp contact via thermal imaging. In *Computer Vision and Pattern Recognition (CVPR)*. 8709–8719.
- Samarth Brahmabhatt, Chengcheng Tang, Christopher D Twigg, Charles C Kemp, and James Hays. 2020. ContactPose: A dataset of grasps with object contact and hand pose. In *European Conference on Computer Vision (ECCV)*. Springer, 361–378.
- Jona Braun, Sammy Christen, Muhammed Kocabas, Emre Aksan, and Otmar Hilliges. 2024. Physically Plausible Full-Body Hand-Object Interaction Synthesis. In *International Conference on 3D Vision (3DV)*.
- Yu-Wei Chao, Wei Yang, Yu Xiang, Pavlo Molchanov, Ankur Handa, Jonathan Tremblay, Yashraj S. Narang, Karl Van Wyk, Umar Iqbal, Stan Birchfield, Jan Kautz, and Dieter Fox. 2021. DexYCB: A Benchmark for Capturing Hand Grasping of Objects. In *Computer Vision and Pattern Recognition (CVPR)*.
- Sirui Chen, Albert Wu, and C. Karen Liu. 2023b. Synthesizing Dexterous Nonprehensile Pregrasp for Ungraspable Objects. In *ACM SIGGRAPH 2023 Conference Proceedings (Los Angeles, CA, USA) (SIGGRAPH '23)*. Association for Computing Machinery, New York, NY, USA, Article 10, 10 pages. <https://doi.org/10.1145/3588432.3591528>
- Xin Chen, Biao Jiang, Wen Liu, Zilong Huang, Bin Fu, Tao Chen, and Gang Yu. 2023a. Executing your Commands via Motion Diffusion in Latent Space. In *Proceedings of the IEEE/CVF Conference on Computer Vision and Pattern Recognition*. 18000–18010.
- Min Jin Chong and David Forsyth. 2020. Effectively unbiased fid and inception score and where to find them. In *Proceedings of the IEEE/CVF conference on computer vision and pattern recognition*. 6070–6079.
- Sammy Christen, Muhammed Kocabas, Emre Aksan, Jemin Hwangbo, Jie Song, and Otmar Hilliges. 2022. D-Grasp: Physically Plausible Dynamic Grasp Synthesis for Hand-Object Interactions. In *Computer Vision and Pattern Recognition (CVPR)*.
- Jia Deng, Wei Dong, Richard Socher, Li-Jia Li, Kai Li, and Li Fei-Fei. 2009. Imagenet: A large-scale hierarchical image database. In *Computer Vision and Pattern Recognition (CVPR)*. Ieee, 248–255.
- Prafulla Dhariwal and Alexander Nichol. 2021. Diffusion models beat gans on image synthesis. *Advances in neural information processing systems* 34 (2021), 8780–8794.
- Christian Diller and Angela Dai. 2023. CG-HOI: Contact-Guided 3D Human-Object Interaction Generation. *arXiv preprint arXiv:2311.16097* (2023).
- Zicong Fan, Maria Pirelli, Maria Eleni Kadoglou, Muhammed Kocabas, Xu Chen, Michael J Black, and Otmar Hilliges. 2024. HOLD: Category-agnostic 3D Reconstruction of Interacting Hands and Objects from Video. In *Computer Vision and Pattern Recognition (CVPR)*.
- Zicong Fan, Omid Taheri, Dimitrios Tzionas, Muhammed Kocabas, Manuel Kaufmann, Michael J. Black, and Otmar Hilliges. 2023. ARCTIC: A Dataset for Dexterous Bimanual Hand-Object Manipulation. In *Computer Vision and Pattern Recognition (CVPR)*.
- Joseph L Fleiss. 1971. Measuring nominal scale agreement among many raters. *Psychological bulletin* (1971).
- Guillermo Garcia-Hernando, Edward Johns, and Tae-Kyun Kim. 2020. Physics-based dexterous manipulations with estimated hand poses and residual reinforcement learning. In *International Conference on Robotics and Automation (ICRA)*. IEEE, 9561–9568.
- Anindita Ghosh, Rishabh Dabral, Vladislav Golyanik, Christian Theobalt, and Philipp Slusallek. 2023. IMoS: Intent-Driven Full-Body Motion Synthesis for Human-Object Interactions. In *Eurographics*.
- Chuan Guo, Xinxin Zuo, Sen Wang, Shihao Zou, Qingyao Sun, Annan Deng, Minglun Gong, and Li Cheng. 2020. Action2motion: Conditioned generation of 3d human motions. In *Proceedings of the 28th ACM International Conference on Multimedia*. 2021–2029.
- Shreyas Hampali, Mahdi Rad, Markus Oberweger, and Vincent Lepetit. 2020. HOnnotate: A method for 3D Annotation of Hand and Object Poses. In *Computer Vision and Pattern Recognition (CVPR)*.
- Mohamed Hassan, Yunrong Guo, Tingwu Wang, Michael Black, Sanja Fidler, and Xue Bin Peng. 2023. Synthesizing Physical Character-scene Interactions. In *International Conference on Computer Graphics and Interactive Techniques (SIGGRAPH)*.
- Yana Hasson, Gül Varol, Dimitris Tzionas, Igor Kalevatykh, Michael J. Black, Ivan Laptev, and Cordelia Schmid. 2019. Learning joint reconstruction of hands and manipulated objects. In *Computer Vision and Pattern Recognition (CVPR)*.
- Jonathan Ho, Ajay Jain, and Pieter Abbeel. 2020. Denoising diffusion probabilistic models. *Advances in neural information processing systems* 33 (2020), 6840–6851.
- Jonathan Ho and Tim Salimans. 2022. Classifier-free diffusion guidance. *NeurIPS 2021 Workshop on Deep Generative Models and Downstream Applications*: (2022).
- Jonathan Ho, Tim Salimans, Alexey Gritsenko, William Chan, Mohammad Norouzi, and David J Fleet. 2022. Video diffusion models. *arXiv:2204.03458* (2022).
- Siyuan Huang, Zan Wang, Puhao Li, Baoxiong Jia, Tengyu Liu, Yixin Zhu, Wei Liang, and Song-Chun Zhu. 2023. Diffusion-based Generation, Optimization, and Planning in 3D Scenes. *arXiv:2301.06015 [cs.CV]*
- Sadeep Jayasumana, Srikumar Ramalingam, Andreas Veit, Daniel Glasner, Ayan Chakrabarti, and Sanjiv Kumar. 2023. Rethinking FID: Towards a Better Evaluation Metric for Image Generation. *arXiv:2401.09603 [cs.CV]*
- Korrawe Karunratanakul, Konpat Preechakul, Emre Aksan, Thabo Beeler, Supasorn Suwajanakorn, and Siyu Tang. 2024. Optimizing Diffusion Noise Can Serve As Universal Motion Priors. In *Computer Vision and Pattern Recognition (CVPR)*.
- Korrawe Karunratanakul, Konpat Preechakul, Supasorn Suwajanakorn, and Siyu Tang. 2023. Guided Motion Diffusion for Controllable Human Motion Synthesis. In *Proceedings of the IEEE/CVF International Conference on Computer Vision*. 2151–2162.
- Korrawe Karunratanakul, Jinlong Yang, Yan Zhang, Michael J Black, Krikamol Muandet, and Siyu Tang. 2020. Grasping field: Learning implicit representations for human grasps. In *2020 International Conference on 3D Vision (3DV)*. IEEE, 333–344.
- Manuel Kaufmann, Velko Vechev, and Dario Mylonopoulos. 2022. *aitviewer*. <https://doi.org/10.5281/zenodo.10013305>
- Zhifeng Kong, Wei Ping, Jiayi Huang, Kexin Zhao, and Bryan Catanzaro. 2021. DiffWave: A Versatile Diffusion Model for Audio Synthesis. In *International Conference on Learning Representations*. <https://openreview.net/forum?id=a-xFK8Ymz5J>
- Taein Kwon, Bugra Tekin, Jan Stühmer, Federica Bogo, and Marc Pollefeys. 2021. H2O: Two Hands Manipulating Objects for First Person Interaction Recognition. In *International Conference on Computer Vision (ICCV)*. 10138–10148.
- Jiye Lee and Hanbyul Joo. 2023. Locomotion-Action-Manipulation: Synthesizing Human-Scene Interactions in Complex 3D Environments. *arXiv:2301.02667 [cs.CV]*
- Rosario Leonardi, Antonino Furnari, Francesco Ragusa, and Giovanni Maria Farinella. 2023. Are Synthetic Data Useful for Egocentric Hand-Object Interaction Detection? An Investigation and the HOI-Synth Domain Adaptation Benchmark. *arXiv preprint arXiv:2312.02672* (2023).
- Jiaman Li, Alexander Clegg, Roozbeh Mottaghi, Jiajun Wu, Xavier Puig, and C Karen Liu. 2023. Controllable Human-Object Interaction Synthesis. *arXiv preprint arXiv:2312.03913* (2023).
- Quanzhou Li, Jingbo Wang, Chen Change Loy, and Bo Dai. 2024b. Task-oriented human-object interactions generation with implicit neural representations. In *Proceedings of the IEEE/CVF Winter Conference on Applications of Computer Vision*. 3035–3044.
- Yuyang Li, Bo Liu, Yiran Geng, Puhao Li, Yaodong Yang, Yixin Zhu, Tengyu Liu, and Siyuan Huang. 2024a. Grasp multiple objects with one hand. *IEEE Robotics and Automation Letters* (2024).
- Tengyu Liu, Zeyu Liu, Ziyuan Jiao, Yixin Zhu, and Song-Chun Zhu. 2021. Synthesizing diverse and physically stable grasps with arbitrary hand structures using differentiable force closure estimator. *IEEE Robotics and Automation Letters* 7, 1 (2021), 470–477.
- Xueyi Liu and Li Yi. 2024. GeneOH Diffusion: Towards Generalizable Hand-Object Interaction Denoising via Denoising Diffusion. In *The Twelfth International Conference on Learning Representations*.
- Yunze Liu, Yun Liu, Che Jiang, Kangbo Lyu, Weikang Wan, Hao Shen, Boqiang Liang, Zhoujie Fu, He Wang, and Li Yi. 2022. HOI4D: A 4D Egocentric Dataset for Category-Level Human-Object Interaction. In *Computer Vision and Pattern Recognition (CVPR)*. 21013–21022.
- Zhengyi Luo, Ryo Hachiuma, Ye Yuan, and Kris Kitani. 2021. Dynamics-regulated kinematic policy for egocentric pose estimation. *Advances in Neural Information Processing Systems* 34 (2021), 25019–25032.
- Naureen Mahmood, Nima Ghorbani, Nikolaus F. Troje, Gerard Pons-Moll, and Michael J. Black. 2019. AMASS: Archive of Motion Capture as Surface Shapes. In *International Conference on Computer Vision*. 5442–5451.
- Priyanka Mandikal and Kristen Grauman. 2021. Learning Dexterous Grasping with Object-Centric Visual Affordances. In *International Conference on Robotics and Automation (ICRA)*.
- Alexander Quinn Nichol and Prafulla Dhariwal. 2021. Improved denoising diffusion probabilistic models. In *International Conference on Machine Learning*. PMLR, 8162–8171.
- Atsuhiko Noguchi and Tatsuya Harada. 2019. Image generation from small datasets via batch statistics adaptation. In *Proceedings of the IEEE/CVF International Conference on Computer Vision*. 2750–2758.
- Georgios Pavlakos, Dandan Shan, Ilija Radosavovic, Angjoo Kanazawa, David Fouhey, and Jitendra Malik. 2024. Reconstructing Hands in 3D with Transformers. In *Computer Vision and Pattern Recognition (CVPR)*.
- Xiaogang Peng, Yiming Xie, Zizhao Wu, Varun Jampani, Deqing Sun, and Huaizu Jiang. 2023. HOI-Diff: Text-Driven Synthesis of 3D Human-Object Interactions using Diffusion Models. *arXiv preprint arXiv:2312.06553* (2023).
- Sergey Prokudin, Christoph Lassner, and Javier Romero. 2019. Efficient learning on point clouds with basis point sets. In *Computer Vision and Pattern Recognition (CVPR)*. 4332–4341.
- Yuzhe Qin, Yueh-Hua Wu, Shaowei Liu, Hanwen Jiang, Ruihan Yang, Yang Fu, and Xiaolong Wang. 2021. DexMV: Imitation Learning for Dexterous Manipulation from Human Videos. *arXiv preprint arXiv:2108.05877* (2021).
- Alec Radford, Jong Wook Kim, Chris Hallacy, Aditya Ramesh, Gabriel Goh, Sandhini Agarwal, Girish Sastry, Amanda Askell, Pamela Mishkin, Jack Clark, et al. 2021.

- Learning transferable visual models from natural language supervision. In *International conference on machine learning*. PMLR, 8748–8763.
- Aravind Rajeswaran, Vikash Kumar, Abhishek Gupta, Giulia Vezzani, John Schulman, Emanuel Todorov, and Sergey Levine. 2018. Learning Complex Dexterous Manipulation with Deep Reinforcement Learning and Demonstrations. In *Robotics: Science and Systems (RSS)*.
- Robin Rombach, Andreas Blattmann, Dominik Lorenz, Patrick Esser, and Björn Ommer. 2022. High-resolution image synthesis with latent diffusion models. In *Proceedings of the IEEE/CVF conference on computer vision and pattern recognition*. 10684–10695.
- Javier Romero, Dimitrios Tzionas, and Michael J. Black. 2017. Embodied Hands: Modeling and Capturing Hands and Bodies Together. *Transactions on Graphics (TOG)* 36, 6 (Nov. 2017).
- Qijin She, Ruizhen Hu, Juzhan Xu, Min Liu, Kai Xu, and Hui Huang. 2022. Learning High-DOF Reaching-and-Grasping via Dynamic Representation of Gripper-Object Interaction. *Transactions on Graphics (TOG)* 41, 4 (2022), 97:1–97:14.
- Soshi Shimada, Franziska Mueller, Jan Bednarik, Bardia Doosti, Bernd Bickel, Danhang Tang, Vladislav Golyanik, Jonathan Taylor, Christian Theobalt, and Thabo Beeler. 2023. Macs: Mass conditioned 3d hand and object motion synthesis. *arXiv preprint arXiv:2312.14929* (2023).
- Nina Shvetsova, Anna Kukleva, Bernt Schiele, and Hilde Kuehne. 2023. In-Style: Bridging Text and Uncurated Videos with Style Transfer for Text-Video Retrieval. *International Conference on Computer Vision (ICCV)* (2023).
- Jascha Sohl-Dickstein, Eric Weiss, Niru Maheswaranathan, and Surya Ganguli. 2015. Deep unsupervised learning using nonequilibrium thermodynamics. In *International conference on machine learning*. PMLR, 2256–2265.
- Omid Taheri, Vasileios Choutas, Michael J. Black, and Dimitrios Tzionas. 2022. GOAL: Generating 4D Whole-Body Motion for Hand-Object Grasping. In *Computer Vision and Pattern Recognition (CVPR)*. <https://goal.is.tue.mpg.de>
- Omid Taheri, Nima Ghorbani, Michael J. Black, and Dimitrios Tzionas. 2020. GRAB: A Dataset of Whole-Body Human Grasping of Objects. In *European Conference on Computer Vision (ECCV)*. <https://grab.is.tue.mpg.de>
- Omid Taheri, Yi Zhou, Dimitrios Tzionas, Yang Zhou, Duygu Ceylan, Soren Pirk, and Michael J. Black. 2024. GRIP: Generating Interaction Poses Using Latent Consistency and Spatial Cues. In *International Conference on 3D Vision (3DV)*. <https://grip.is.tue.mpg.de>
- Purva Tendulkar, Didac Surís, and Carl Vondrick. 2023. FLEX: Full-Body Grasping Without Full-Body Grasps. In *Computer Vision and Pattern Recognition (CVPR)*.
- Guy Tevet, Sigal Raab, Brian Gordon, Yoni Shafir, Daniel Cohen-or, and Amit Haim Bermano. 2023. Human Motion Diffusion Model. In *The Eleventh International Conference on Learning Representations*. <https://openreview.net/forum?id=SJ1kSyO2jwu>
- Weikang Wan, Haoran Geng, Yun Liu, Zikang Shan, Yaodong Yang, Li Yi, and He Wang. 2023. UniDexGrasp++: Improving Dexterous Grasping Policy Learning via Geometry-aware Curriculum and Iterative Generalist-Specialist Learning. *arXiv preprint arXiv:2304.00464* (2023).
- Jingbo Wang, Sijie Yan, Bo Dai, and Dahua Lin. 2021. Scene-aware generative network for human motion synthesis. In *Computer Vision and Pattern Recognition (CVPR)*. 12206–12215.
- Ruicheng Wang, Jialiang Zhang, Jiayi Chen, Yinzhen Xu, Puhao Li, Tengyu Liu, and He Wang. 2023. DexGraspNet: A Large-Scale Robotic Dexterous Grasp Dataset for General Objects Based on Simulation. In *International Conference on Robotics and Automation (ICRA)*. IEEE, 11359–11366.
- Yan Wu, Jiahao Wang, Yan Zhang, Siwei Zhang, Otmar Hilliges, Fisher Yu, and Siyu Tang. 2022. SAGA: Stochastic Whole-Body Grasping with Contact. In *Proceedings of the European Conference on Computer Vision (ECCV)*.
- Sirui Xu, Zhengyuan Li, Yu-Xiong Wang, and Liang-Yan Gui. 2023a. InterDiff: Generating 3D Human-Object Interactions with Physics-Informed Diffusion. In *International Conference on Computer Vision (ICCV)*.
- Yinzhen Xu, Weikang Wan, Jialiang Zhang, Haoran Liu, Zikang Shan, Hao Shen, Ruicheng Wang, Haoran Geng, Yijia Weng, Jiayi Chen, et al. 2023b. UniDexGrasp: Universal Robotic Dexterous Grasping via Learning Diverse Proposal Generation and Goal-Conditioned Policy. In *Computer Vision and Pattern Recognition (CVPR)*. 4737–4746.
- Lixin Yang, Kailin Li, Xinyu Zhan, Fei Wu, Anran Xu, Liu Liu, and Cewu Lu. 2022. OakInk: A Large-Scale Knowledge Repository for Understanding Hand-Object Interaction. In *Computer Vision and Pattern Recognition (CVPR)*.
- Ling Yang, Zhilong Zhang, Yang Song, Shenda Hong, Runsheng Xu, Yue Zhao, Wentao Zhang, Bin Cui, and Ming-Hsuan Yang. 2023. Diffusion models: A comprehensive survey of methods and applications. *Comput. Surveys* 56, 4 (2023), 1–39.
- Yufei Ye, Poorvi Hebbar, Abhinav Gupta, and Shubham Tulsiani. 2023a. Diffusion-Guided Reconstruction of Everyday Hand-Object Interaction Clips. In *International Conference on Computer Vision (ICCV)*.
- Yufei Ye, Xueting Li, Abhinav Gupta, Shalini De Mello, Stan Birchfield, Jiaming Song, Shubham Tulsiani, and Sifei Liu. 2023b. Affordance Diffusion: Synthesizing Hand-Object Interactions. In *Computer Vision and Pattern Recognition (CVPR)*.
- Yuting Ye and C Karen Liu. 2012. Synthesis of detailed hand manipulations using contact sampling. *Transactions on Graphics (TOG)* 31, 4 (2012), 1–10.
- Ye Yuan, Jiaming Song, Umar Iqbal, Arash Vahdat, and Jan Kautz. 2023. PhysDiff: Physics-Guided Human Motion Diffusion Model. In *International Conference on Computer Vision (ICCV)*.
- Xinyu Zhan, Lixin Yang, Yifei Zhao, Kangrui Mao, Hanlin Xu, Zenan Lin, Kailin Li, and Cewu Lu. 2024. OAKINK2: A Dataset of Bimanual Hands-Object Manipulation in Complex Task Completion. In *Computer Vision and Pattern Recognition (CVPR)*. 445–456.
- Hui Zhang, Sammy Christen, Zicong Fan, Otmar Hilliges, and Jie Song. 2024a. GraspXL: Generating Grasping Motions for Diverse Objects at Scale. *European Conference on Computer Vision (ECCV)* (2024).
- Hui Zhang, Sammy Christen, Zicong Fan, Luo Cheng Zheng, Jemin Hwangbo, Jie Song, and Otmar Hilliges. 2024b. ArtiGrasp: Physically Plausible Synthesis of Bi-Manual Dexterous Grasping and Articulation. In *International Conference on 3D Vision (3DV)*.
- He Zhang, Yuting Ye, Takaaki Shiratori, and Taku Komura. 2021. Manipnet: neural manipulation synthesis with a hand-object spatial representation. *Transactions on Graphics (TOG)* 40, 4 (2021), 1–14.
- Lvmin Zhang, Anyi Rao, and Maneesh Agrawala. 2023. Adding conditional control to text-to-image diffusion models. In *Proceedings of the IEEE/CVF International Conference on Computer Vision*. 3836–3847.
- Mingyuan Zhang, Zhongang Cai, Liang Pan, Fangzhou Hong, Xinying Guo, Lei Yang, and Ziwei Liu. 2022b. MotionDiffuse: Text-Driven Human Motion Generation with Diffusion Model. *arXiv preprint arXiv:2208.15001* (2022).
- Xiaohan Zhang, Bharat Lal Bhatnagar, Sebastian Starke, Vladimir Guzov, and Gerard Pons-Moll. 2022a. COUCH: Towards Controllable Human-Chair Interactions. (October 2022).
- Juntian Zheng, Qingyuan Zheng, Lixing Fang, Yun Liu, and Li Yi. 2023. CAMS: CAnonicalized Manipulation Spaces for Category-Level Functional Hand-Object Manipulation Synthesis. In *Proceedings of the IEEE/CVF Conference on Computer Vision and Pattern Recognition*. 585–594.
- Keyang Zhou, Bharat Lal Bhatnagar, Jan Eric Lenssen, and Gerard Pons-Moll. 2022. Toch: Spatio-temporal object-to-hand correspondence for motion refinement. In *European Conference on Computer Vision*. Springer, 1–19.
- Yi Zhou, Connelly Barnes, Jingwan Lu, Jimei Yang, and Hao Li. 2019. On the continuity of rotation representations in neural networks. In *Proceedings of the IEEE/CVF Conference on Computer Vision and Pattern Recognition*. 5745–5753.

A Implementation Details

While we experiment with a transformer backbone as proposed in MDM [Tevet et al. 2023], DiffH₂O’s main architecture is based on UNet with Adaptive Group Normalization (AdaGN) which was originally proposed in [Dhariwal and Nichol 2021] and also adapted in [Karunratanakul et al. 2023] for sequence prediction tasks. We adapt this network architecture for our two-stage design, that involves grasping and interaction diffusion models. We provide the hyperparameter settings used in our architecture in Table 6.

B Experimental Details

B.1 Obtaining Grasp References

As mentioned in the main part of the paper, we show three different ways grasp references can be obtained, namely via existing datasets, pose estimation, or grasp synthesis. Note that these procedures for acquiring hand pose references have already been established in related works [Christen et al. 2022; Xu et al. 2023b], albeit for the sole purpose of grasping and not interaction.

Hand-Object Datasets. The most straightforward way to attain grasp references is to make use of existing hand-object datasets (see Sec. 2). There are some single frame datasets like ObMan [Hasson et al. 2019] or AffordPose [Ye et al. 2023b] that could be directly used as grasp references. However, most existing datasets contain sequential data, hence, we need to identify which frames are potential candidates for hand-object grasps. In our paper, we run guidance experiments on our test split of the GRAB dataset [Taheri et al. 2020]. To acquire suitable frames for guidance, we apply the heuristics described in Sec. 4.2.1. In this case, we can directly use the preprocessed data from GRAB as single keyframes for guidance.

Image-Based Pose Estimation. For this experiment, we need to extract the grasp references from images. We run an image-based pose estimator [Pavlakos et al. 2024] on single images from HO3D [Hampali et al. 2020] to obtain object-relative hand poses. In this experiment, we focus on extracting a single hand pose from the image. Please note that we assume the object mesh to be known and at a normalized position to be suitable for our experiments. Given the object-relative hand pose, we need to make three modifications to convert it to the same input space our model has. First, we have to compute the features for our approximated signed-distance space by finding the closest vertex on the object mesh for each joint position. Second, we convert the hand pose from joint angle space to MANO’s PCA space. Lastly, because the GRAB dataset is normalized to approach objects from one direction, we have to adjust the orientation of the hand and object to roughly be in line with this direction. This could be alleviated by adding data augmentation to the training data in the future. We also leave exploring object mesh reconstruction for future work, for example, by utilizing methods that reconstruct the object mesh along with the hand pose estimation [Fan et al. 2024].

Grasp Synthesis. In this experiment, we use a grasp synthesis method, GraspXL [Zhang et al. 2024a], to obtain grasp references for guidance. To this end, we run GraspXL on several objects to obtain grasping motions. As we only require one frame for the guidance, we take the last frame of the grasping motion as the keyframe. Since

GraspXL allows conditioning on approaching direction, we select grasps whose approaching direction aligns with the GRAB dataset. Again, we compute the approximated signed distance by finding the closest vertex on the object mesh for each joint position and convert the hand pose from joint angle to MANO PCA space. There is no further conversion needed, as the object poses are already normalized. Similar to the experiment with hand poses from images, we only acquire an object-relative grasp and its respective features for one hand.

B.2 Additional Motion Feature Evaluation Metrics.

For completion, we also provide metrics based on an action recognition classifier following previous motion synthesis works [Ghosh et al. 2023; Tevet et al. 2023].

Action Recognition Accuracy (AR). Given a pretrained classifier, we input motions generated by DiffH₂O as well as our baselines and report top-1 percentage accuracy. The recognition accuracy indicates the correlation of the action type and the motion.

Diversity (DIV). We compute the diversity score by computing the variance of the features extracted from the action classifier across all action categories. Given a set of features extracted from generated motions across all action categories, two subsets with the same size, N , are randomly sampled. These features are denoted as $\{\mathbf{v}_1, \mathbf{v}_2, \dots, \mathbf{v}_N\}$ for the first subset and $\{\mathbf{v}'_1, \mathbf{v}'_2, \dots, \mathbf{v}'_N\}$ for the second subset. With $N = 200$, the diversity is defined as

$$\text{DIV} = \frac{1}{N} \sum_{i=1}^N \|\mathbf{v}_i - \mathbf{v}'_i\| \quad (7)$$

Multimodality (MM). Different from diversity, multimodality computes variance only within a specific action. An overall score is attained based on averaging the variances across all action types.

Fréchet Inception Distance (FID). FID is computed based on the (Fréchet) distance of the features of real ground-truth motions and generated motions. It has the assumption that the features computed from the real data and synthesized data have a Gaussian distribution. Earlier work demonstrated that for small sample sizes, FID metric is biased and not stable [Noguchi and Harada 2019].

Kernel Inception Distance (KID). KID metric relaxes the Gaussianity assumption and aims to improve upon FID. It measures the squared Maximum Mean Discrepancy (MMD) between the feature representations of the real and generated samples using a polynomial kernel. This metric has been found to be more robust when the sample size is small [Noguchi and Harada 2019].

B.3 Metrics - Training the Action Classifier.

To provide motion feature metrics (see Sec. B.2) based on an action classifier, we train a standard RNN action recognition classifier on the GRAB dataset. We use the final layer of the classifier as the motion feature extractor for calculating action recognition accuracies as well as diversity (DIV) and multimodality (MM) scores, following [Ghosh et al. 2023] and [Guo et al. 2020]. We employ the online available code from IMoS and use the same network architecture and parameters to train our model.

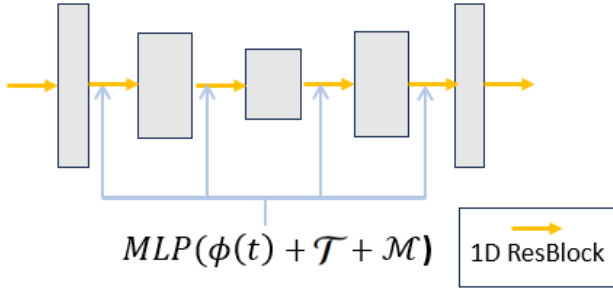


Fig. 6. **Overview of the diffusion architecture.** Our pipeline relies on a UNet block and processes three input signals: the time step $\phi(t)$, a text-prompt embedding \mathcal{T} and an object shape encoding \mathcal{M} . The time step is encoded using sinusoidal functions, the text-prompt embedding is generated by the CLIP text encoder model and the object encoding is obtained from BPS [Prokudin et al. 2019]. Similarly to [Karunratanakul et al. 2023], we use Adaptive Group normalization in 1D block

Parameter	Grasping Model	Interaction Model
Batch size	32	32
Base channels	256	512
Latent dimension	256	512
Channel multipliers	(1, 1, 1)	(2, 2, 2, 2)
β scheduler	Cosine [Nichol and Dhariwal 2021]	
Learning rate	1e-4	1e-4
Optimizer	AdamW (wd = 1e-2)	
Training T	400	
Diffusion loss	ϵ prediction	\mathbf{x}_0 prediction
Diffusion var.	Fixed small $\tilde{\beta}_t = \frac{1-\alpha_{t-1}}{1-\alpha_t} \beta_t$	
Model avg. beta	0.9999	

Table 6. **Network architecture.** Model and hyperparameters of DiffH₂O

B.4 Annotation Examples

We provide a few examples of our textual annotations in Table 10. Please see our code release for the entire set of annotations*.

B.5 Visualization Pipeline.

We use AITViewer [Kaufmann et al. 2022] to visualize motions synthesized by DiffH₂O as well as our baselines. IMoS synthesizes 15 frames of human-object interactions. They determine the hand which is in contact with the object according to GT, which can lead to a jump of the object from one hand to the other for certain actions. To make the frame rates comparable with DiffH₂O, we upsample the synthesis results of IMoS to 75 frames using spherical interpolation. Therefore, this jump may result in an artifact in which the object is floating from one hand to another.

*The code and data will be available here: <https://diffh2o.github.io>

C Additional Experiments

C.1 Action Recognition Experiments

Training action classifier on the whole GRAB data. IMoS [Ghosh et al. 2023] reports results using the whole dataset to train the action classifier on ground-truth motions and testing on the synthesized actions. Since their model initializes the sequences with ground-truth from the test data, this could positively bias their scores. Therefore, we omit test data from training, in our analysis in Table 1 of the main paper, both for our approach and IMoS. We show however in this supplemental material (Table 7) that our model is still able to outperform IMoS even when all the GRAB data, including test data, is included in training the classifier. This is a setup which is more favorable for IMoS as the first frames of synthesized IMoS motion is taken from the test data. This re-confirms the ability of our method to encode diverse motion features that represents realistic hand-object interactions. Furthermore, we train two models, one that uses only hand 3D joints as input and another incorporating object 3D position as additional input. We demonstrate that DiffH₂O’s synthesized object motions outperform IMoS in both settings. This confirms the benefits of jointly modeling hand-object motion instead of decoupling it into separate components. Note also that as expected, the classifier can correctly identify all test sequences of the real mocap data, since it has seen the test data during training in the IMoS setting.

FID and KID metrics. It’s been shown by earlier studies [Noguchi and Harada 2019], [Jayasumana et al. 2023], [Chong and Forsyth 2020] that Fréchet Inception Distance (FID) metric is biased and not stable for calculating the distances for small datasets. Since the GRAB subject split only contains 144 motions, in addition to FID, we also report the more stable Kernel Inception Distance (KID) metric which provides more reliable scores with fewer samples (Table 8). Table 8 also includes the standard deviations for the multimodality and diversity metrics based upon 20 repetitions of the evaluation.

Full-sequence training. Given an initial pose of the grasp moment, IMoS only synthesizes interaction sequences. To compare our results to IMoS in Table 1 of the main paper, we evaluated our models only on the interaction sequence part of the synthesis. In Table 9, we also provide diversity, multimodality, FID, KID and action recognition scores computed over the full sequence including grasp and interaction stages. We compare our results against motions from motion capture and observe that we can achieve scores similar to real mocap, which demonstrates our capability to synthesize realistic hand-object interactions.

C.2 Analysis on Generalizability

When we analyze per-unseen-object performance on GRAB, our method effectively generalizes to unseen objects with various sizes and shapes (e.g., apple, clock, train, elephant, mug, etc.). We also evaluated the influence of object scale on three test objects by using objects of the same shape but different scales during training: our model performs well on medium cylinder and large torus (584cm³), but faces challenges on small pyramid (64cm³, video: 04.40, low contact-ratio). The average bounding-box volumes for our train and test sets are 741cm³ and 625cm³, respectively. In conclusion, our

	Method	Hand AR (\uparrow)	Hand+Object AR (\uparrow)	DIV (\rightarrow)	MM (\rightarrow)	KID (\downarrow)	FID (\downarrow)
Unseen subject split	Real Mocap	1.0	1.0	1.1358 \pm 0.0164	0.3105 \pm 0.0163	-	-
	IMoS [Ghosh et al. 2023]	0.7017	0.6754	1.1053 \pm 0.0128	0.2882 \pm 0.0114	0.005811	0.6267
	DiffH ₂ O	0.8125	0.9028	1.1440\pm0.0115	0.3176\pm0.0127	0.005346	0.8342
Unseen object split	Real Mocap	1.0	1.0	1.1324 \pm 0.0119	0.2355 \pm 0.0044	-	-
	IMoS* [Ghosh et al. 2023]	0.7161	0.8000	1.1173 \pm 0.0112	0.2513\pm0.0104	0.006038	0.7101
	DiffH ₂ O	0.7836	0.8125	1.1225\pm0.0120	0.2174 \pm 0.0074	0.005494	0.8821

Table 7. **Action feature based metrics using all training data.** We report action feature based metrics using action recognition models trained on all of the GRAB training data following the protocol of [Ghosh et al. 2023]. We either use a subject-based split (top 3 rows) or an object-based split (bottom 3 rows). \downarrow denotes lower values are better, and \rightarrow denotes values closer to the ground-truth are better. Our results achieves state-of-the-art accuracy across different metrics.

	Method	DIV (\rightarrow)	MM (\rightarrow)	KID (\downarrow)	FID (\downarrow)
Unseen subject split	Real Mocap	1.0632 \pm 0.0131	0.2155 \pm 0.0091	-	-
	IMoS [Ghosh et al. 2023]	1.0237 \pm 0.0158	0.2538\pm0.0103	0.008065	0.6267
	DiffH ₂ O	1.0757\pm0.0129	0.3037 \pm 0.0079	0.006697	0.8342
Unseen object split	Real Mocap	1.0757 \pm 0.0129	0.2002 \pm 0.0063	-	-
	IMoS* [Ghosh et al. 2023]	1.0471 \pm 0.0129	0.2202\pm0.0093	0.008641	0.6593
	DiffH ₂ O	1.0942\pm0.0125	0.2307 \pm 0.0060	0.007503	0.8425

Table 8. **Details of the quantitative analysis with action feature based metrics.** We provide further details for the quantitative analysis in Table 1 of the main paper and report standard deviations of multimodality and diversity metrics as well as FID and KID scores. The results here are obtained using action recognition models trained on hand pose data of the respective training splits as indicated in the first column. We either use a subject-based split (top 3 rows) or an object-based split (bottom 3 rows). For IMoS, we use the same pretrained model, which is trained on unseen subject split, across all our experiments (unseen subject and unseen object splits) due to difficulties in reproducing training performance for the unseen object split (indicated with a * in the table, IMoS*). Therefore IMoS* sees a part of the unseen object test split during training the model which positively biases their score. \downarrow denotes lower values are better, and \rightarrow denotes values closer to the ground-truth (real mocap) are better. Our results achieves state-of-the-art accuracy across different metrics.

Method	Hand Act. Rec. Accuracy (\uparrow)	Hand+Object Act. Rec. Accuracy (\uparrow)	DIV (\rightarrow)	MM (\rightarrow)	KID (\downarrow)	FID (\downarrow)
Real Mocap (Full-sequence)	1.0	1.0	1.0983 \pm 0.0059	0.2235 \pm 0.0042	-	-
DiffH ₂ O (Full-sequence)	0.7720	0.8031	1.0948 \pm 0.0120	0.1555 \pm 0.0057	0.0067	0.7993

Table 9. **Action feature based metrics on full sequence synthesis.** We report action feature based metrics on our unseen object split using action recognition models trained on full sequences instead of only post-grasp data as in [Ghosh et al. 2023]. \downarrow denotes lower values are better, and \rightarrow denotes values closer to the ground-truth are better. Our results achieves state-of-the-art accuracy across different metrics.

model adapts well to unseen shapes and a wide range of sizes, but largely out-of-distribution sizes (e.g., also large_cracker_box from HO3D: 2208cm³) lead to less favorable physics metrics.

C.3 Discussion on Grasp References

Here we provide a more detailed discussion about the role of grasp references that are used for guidance.

Strengths: Grasp guidance is a technique to increase the controllability and improve generalization on unseen objects if grasp references are available. Note, however, that our model without guidance already significantly outperforms baselines (cf. Table 1 in the main paper), making it an ideal tool for potential downstream use cases. Grasp guidance yields better generalization (e.g., less interpenetration as shown in Table 2 in the main paper), because it provides a signal to the diffusion model about how an object should

be grasped. Especially for unseen object geometry, this can serve as important information about feasible grasping poses of the hand. One of the other main advantages of grasp guidance is that it allows defining the grasping hand(s) on the object, which may be important if rich textual annotations such as the ones presented in Sec. 4.4 are not available.

Weaknesses and Failures: Grasp guidance faces an important trade-off: while the signal can be helpful for object generalization and controllability of handedness, it requires access to single hand-object poses. We detail in Section B.1 how such grasp references can be obtained. Hence, there are conversion steps that are necessary to make guidance work on unseen object geometry, which require some manual effort. For instance, due to the small dataset size of GRAB and the similar approaching direction for all objects, an alignment step is necessary to make the guidance signal useful. In the

Object Name	Annotation
camera	The person uses their left hand to pick up the camera, brings it closer to their eyes to take a photo, and then places it back on the table with their right hand.
stapler	The person repeatedly picks up and places the stapler on the table always with their right hand.
mouse	The person picks up the mouse with their right hand, passes it to someone on their right below chest level, and then places it back on the table with their right hand.
alarm clock	The person repeatedly picks up the alarm clock with their right hand, lifts it, and places it back on the table with their right hand.
duck	Using the right hand, the person picks up the duck, examines it closely, and then places the duck back down on the table.
bowl	The person picks up the bowl with both hands, drinks from it, and places it back on the table with both hands.
headphones	The person picks up the headphones with their left hand, puts them on with both hands, and places them on the table with both hands.
banana	The person picks up the banana with their right hand, passes it to their left hand, then hands it to someone on their left side at shoulder level with their left hand, and finally places it back on the table with their right hand.

Table 10. Examples of our textual sequence descriptions

future, larger dataset distributions or additional data augmentation techniques may help alleviate this. Furthermore, as our model is conditioned on both the text description and the grasp guidance, one needs to make sure that the two align: for example, if the grasp reference shows grasping a cup from above, where the prompted action is "drink from the cup", the model is forced to select which signal to follow. In practice, as the guidance is only a weak guidance signal at a single frame, the model will favor the text description over the guidance. Another limiting factor is the size of the unseen objects as discussed in Section C.2. For example, if the object is too large, the target grasp may be reached in the grasping phase, but after imputing the grasping into the interaction stage, the model may neglect the out-of-distribution grasp and output a grasp that displays physical artifacts such as interpenetration.

Overall, grasp guidance is a technique that shows the potential to provide a link between how an object should be grasped and subsequent actions that can be prompted via text. While there are limiting factors in its current state, i.e., manual alignment and matching text prompt with the grasp reference, future work could focus on enhancing existing datasets and using improved guidance techniques [Karunratanakul et al. 2024] to further increase performance.

D Computational Resources

The training of our model takes approximately 48 GPU hours on a single NVIDIA V100. Our model has a throughput of 32 samples per second. The total inference time for 32 samples is approximately 300 seconds.

E Ethical Discussion

Our method uses a generative model, namely diffusion models, to synthesize realistic hand-object motions. While the generated outputs at this point are in 3D and not rendered on photorealistic images with natural backgrounds, such a feature could be added in the future. This may lead to malicious use of our research, such as generating virtual deepfakes. Other downstream applications that could have problematic use cases are robotics, where our generated

data could be used to train robots in handling objects in a desired way. For example, robots could be taught how to handle weapons. Moving forward with the development of our method, we hope that openly discussing the technical details, implementation, and sharing our code will ensure that the technology is well comprehended, accessible to the public and measures to prevent and flag malicious uses are easier to implement.